

University of Ljubljana  
Faculty of **Mathematics and Physics**



Physics department

SEMINAR

# Biased Brownian motion

Author: Mitja Stimulak

Mentor: prof. dr. Rudolf Podgornik

Ljubljana, January 2010

## Abstract

*This seminar is concerned with Biased Brownian motion. Firstly Brownian motion and its properties are described. Then we follow Einsteins steps towards mathematical description of Brownian motion. Brownian motor and a physical principle that explains it, Biased Brownian motion, are introduced next. In the second part we turn our attention to an experiment with a single Brownian particle. There we briefly describe the setup of the experiment and explain how optical trap works. Particle dynamics is discussed with the help of two models one originating from Langevin's equation and another from more general Fokker Planck equation.*

# Contents

<b>1</b>	<b>Introduction</b>	<b>1</b>
<b>2</b>	<b>Brownian motion</b>	<b>2</b>
2.1	Einstein's Explanation of the Brownian Movement - Probability Density Diffusion Equations . . . . .	3
2.2	Brownian motor . . . . .	6
2.3	Biased Brownian motion . . . . .	6
<b>3</b>	<b>Periodic forcing of a Brownian particle</b>	<b>7</b>
3.1	Experimental setup . . . . .	8
3.2	Optical trap . . . . .	8
3.3	Maximum trapping force . . . . .	8
3.4	Particle dynamics . . . . .	9
3.4.1	Phase-Locked regime . . . . .	9
3.4.2	Phase-slip regime . . . . .	11
3.4.3	Diffusive regime . . . . .	11
<b>4</b>	<b>Langevin equation-Stochastic Differential Equations</b>	<b>12</b>
<b>5</b>	<b>Fokker-Planck equation</b>	<b>15</b>
<b>6</b>	<b>Conclusion</b>	<b>17</b>
<b>7</b>	<b>References</b>	<b>17</b>

## 1 Introduction

Brownian motion, in some systems can also be described as noise, is a continuous motion of small particles.

Noise is unavoidable for any system in thermal contact with its surroundings. In technological devices, it is typical to incorporate mechanisms for reducing noise to an absolute minimum. An alternative approach is emerging, however, in which attempts are made to harness noise for useful purposes.

To some extent this can be achieved by inducing some additional potential in system from outside. This process is also known as a Biased Brownian motion.

We are going to study basic principles of Biased Brownian motion. Specifically we are going to look into different regimes of moving of a single Brownian particle that is periodically forced by an optical trap. We will show that these regimes can be derived and described by mathematical formula.

## 2 Brownian motion

First detailed account of Brownian motion was given by eminent botanist Robert Brown in 1827 while studying the plant life of the South Seas. He examined aqueous suspensions of pollen grains of several species under microscope and found out that in all cases the pollen grains were in rapid oscillatory motion.[1]

It is interesting that he initially thought that the movement was peculiar to the male sexual cells of plants. He quickly corrected himself when he observed that the motion was exhibited by both organic and inorganic matter in suspension.[1]

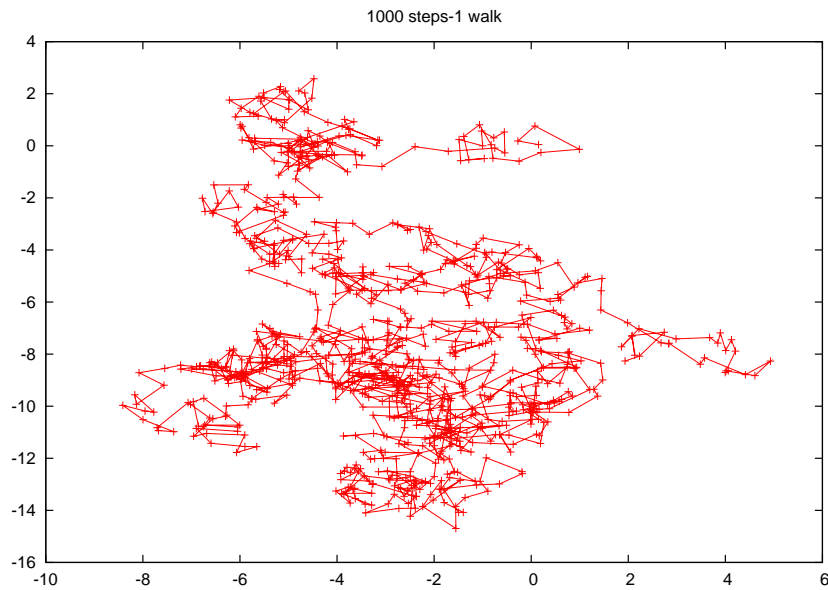


Figure 1: Simulation of a 2D random walk of a Brownian particle. Particle started at the position  $(0,0)$  and made one thousand random steps. At each step the step length  $l$  and the direction of moving  $\varphi$  were randomly chosen.  $-1 < l > 1$  and  $\varphi \in [0, 2\pi]$

Following Brown's work there were many years of speculation as to the cause of the phenomenon, before Einstein made conclusive mathematical predictions of a diffusive effect arising from the random thermal motion of particles in suspension. Before Einsteins work, very detailed experimental investigation was made by Louis Georges Gouy a French physicist. His conclusions may be summarised by the following seven points[1]:

1. The motion is very irregular, composed of translations and rotations, and the trajectory appears to have no tangent.
2. Two particles appear to move independently, even when they approach one another to within a distance less than their diameter.
3. The smaller the particles, the more active the motion.
4. The composition and density of the particles have no effect.
5. The less viscous the fluid, the more active the motion.
6. The higher the temperature, the more active the motion.
7. The motion never ceases.

## 2.1 Einstein's Explanation of the Brownian Movement - Probability Density Diffusion Equations

Einstein's analysis was presented in a series of publications, including his doctoral thesis, that started in 1905 with a paper in the journal *Annalen der Physik*. [2]

Einstein derived his expression for the mean-square displacement of a Brownian particle by means of a diffusion equation which he constructed using the following assumptions: [1]

- (i) Each individual particle executes a motion which is independent of the motion of all other particles in the system.
- (ii) The motion of a particle at one particular instant is independent of the motion of that particle at any other instant, provided the time interval is large enough.

To actually develop the diffusion equation we introduce a time interval  $\tau$ , which is large enough so the second assumption is valid, but small compared to the observable time intervals. Now let's suppose that there are  $\rho$  particles in a liquid per unit volume at  $x$  at time  $t$ . After a time  $\tau$  has elapsed we consider a volume element of the same size at point  $x'$ .

The probability of a particle entering from neighbouring element to  $x'$  is a function of a distance between  $x$  and  $x'$ ,  $\Delta = x' - x$  and  $\tau$ . We denote this probability by  $\Phi = \Phi(\Delta, \tau)$ . Since the particle must come from some volume element, the density at time  $\tau$  is [1]

$$\rho(x, t + \tau) = \int_{-\infty}^{\infty} \rho(x + \Delta, t) \Phi(\Delta, \tau) d\Delta \quad (1)$$

Now positive and negative displacements are equiprobable. We have an unbiased random walk. Thus the function  $\Phi(\Delta, \tau)$  satisfies  $\Phi(\Delta, \tau) = \Phi(-\Delta, \tau)$ . We now suppose that  $\tau$  is very small so that we can expand the left hand side of Eq. (1) in powers of  $\tau$ .

$$\rho(x, t + \tau) = \rho(x, t) + \tau \frac{\partial \rho}{\partial t} + O(\tau^2) \quad (2)$$

Furthermore, we develop  $\rho(x + \Delta, t)$  in powers of small displacement  $\Delta$ , so obtaining

$$\rho(x + \Delta, t) = \rho(x, t) + \Delta \frac{\partial \rho(x, t)}{\partial x} + \frac{\Delta^2}{2!} \frac{\partial^2 \rho(x, t)}{\partial x^2} + \dots \quad (3)$$

The integral equation (1) then becomes:

$$\rho + \tau \frac{\partial \rho}{\partial t} = \rho \int_{-\infty}^{\infty} \Phi(\Delta, \tau) d\Delta + \frac{\partial \rho}{\partial x} \int_{-\infty}^{\infty} \Delta \Phi(\Delta, \tau) d\Delta + \frac{\partial^2 \rho}{\partial x^2} \int_{-\infty}^{\infty} \frac{\Delta^2}{2!} \Phi(\Delta, \tau) d\Delta + \dots \quad (4)$$

Since  $\Phi(\Delta, \tau)$  is a probability density function and  $\Phi(\Delta, \tau) = \Phi(-\Delta, \tau)$  we must have [1]

$$\int_{-\infty}^{\infty} \Phi(\Delta, \tau) d\Delta = 1$$

$$\int_{-\infty}^{\infty} \Delta \Phi(\Delta, \tau) d\Delta = \bar{\Delta} = 0$$

and

$$\int_{-\infty}^{\infty} \Delta^2 \Phi(\Delta, \tau) d\Delta = \overline{\Delta^2},$$

where the overbar denotes the mean over displacement for each particle. We suppose that all higher order terms such as  $\overline{\Delta^4}$  are at least of the order  $\tau^2$ . Hence Eq. (4) simplifies to

$$\tau \frac{\partial \rho}{\partial t} = \frac{\partial^2 \rho}{\partial x^2} \int_{-\infty}^{\infty} \frac{\Delta^2}{2!} \Phi(\Delta, \tau) d\Delta \quad (5)$$

If we set

$$D \equiv \frac{1}{\tau} \int_{-\infty}^{\infty} \frac{\Delta^2}{2!} \Phi(\Delta, \tau) d\Delta = \frac{\overline{\Delta^2}}{2\tau} \quad (6)$$

then Eq. (5) can be written as

$$\frac{\partial \rho}{\partial t} = D \frac{\partial^2 \rho}{\partial x^2}, \quad (7)$$

We developed the diffusion equation in one dimension. Conditions on the solution are

$$\rho(x, 0) = \delta(x) \quad (8)$$

Since  $\rho$  is a probability distribution we also have

$$\int_{-\infty}^{\infty} \rho(x, t) dx = 1 \quad (9)$$

This is well known problem and solution to it in one dimension is

$$\rho(x, t) = \frac{1}{\sqrt{4\pi Dt}} e^{-x^2/4Dt} \quad (10)$$

Einstein determined the translational diffusion coefficient D in terms of molecular qualities as follows.

Let us suppose that the Brownian particles are in a field of force  $F(x)$  (the gravitational field of earth); then the Maxwell-Boltzmann distribution for the configuration of the particles must set in.

$$\rho = \rho_0 e^{-\beta U} \quad (11)$$

If the force is constant, as would be true when gravity acts on the Brownian particles, the potential energy is

$$U = Fx, \quad (12)$$

where we suppose that the particles are so few that their mutual interaction may be neglected (like an "atmosphere" of Brownian particles). Now the velocity of a particle that is in equilibrium under the action of the applied force and viscosity is given by Stokes's law:

$$v = \frac{F}{6\pi\eta a} \quad (13)$$

Number of particles crossing unit area in unit time (current density of particles) is then

$$J = \frac{\rho F}{6\pi\eta a} \quad (14)$$

For a normal diffusion process, particles cannot be created or destroyed, which means the flux of particles into one region must be the sum of particle flux flowing out of the surrounding regions. This can be captured mathematically by the continuity equation.

$$\frac{\partial \rho}{\partial t} + \text{div} J = 0 \quad (15)$$

We combine equations (Eq.7) and (Eq.15) integrate over x and we get

$$-D \frac{\partial \rho}{\partial x} = \frac{\rho F}{6\pi\eta a} \quad (16)$$

From equations (Eq.11) and (Eq.12) we get

$$\frac{1}{\rho} \frac{\partial \rho}{\partial x} = -\frac{F}{k_B T} \quad (17)$$

Comparing equations (Eq.16) and (Eq.17) we obtain

$$D = \frac{k_B T}{6\pi\eta a} \quad (18)$$

or by definition

$$\frac{\Delta^2}{2\tau} \equiv D = \frac{k_B T}{6\pi\eta a} \quad (19)$$

We developed Einstein's formula for the translational diffusion coefficient. One can see that  $\Delta^2 \propto \tau$ .

T is the temperature,  $\eta$  is the viscosity of the liquid and  $a$  is the size of the particle. This equation implies that large particles would diffuse more gradually than molecules, making them easier to measure. Moreover, unlike a ballistic particle such as a billiard ball, the displacement of a Brownian particle would not increase linearly with time but with the square root of time.[3]

Experimental observation confirmed the numerical accuracy of Einstein's theory. This means that we understand Brownian motion just as a consequence of the same thermal motion that causes a gas to exert a pressure on the container that confines it. We understand diffusion in terms of the movements of the individual particles, and can calculate the diffusion coefficient of a molecule if we know its size (or more commonly calculate the size of the molecule after experimental determination of the diffusion coefficient). Thus, Einstein connected the macroscopic process of diffusion with the microscopic concept of thermal motion of individual molecules.[15]

It is interesting to recall that Einstein formulated his theory without having observed Brownian movement, but predicted that such a movement should occur from the standpoint of the kinetic theory of matter.[1]

## 2.2 Brownian motor

Brownian motors are nano-scale or molecular devices, they are used to generate directed motion in space and to do mechanical or electrical work.[9] Many protein-based molecular motors in the cell may in fact be Brownian motors. They use the chemical energy present in ATP to generate fluctuating anisotropic energetic potentials. The anisotropic potentials along the path would bias the motion of a particle (like an ion or polypeptide). The result would essentially be diffusion of a particle whose net motion is strongly biased in one direction.[7]

Distinct from macroscopic, man-made machines, molecular motors work in a very noisy environment, where thermal fluctuations are significant and important to the operation of the motor.[7]

To understand the basic physical principles that govern molecular motors it is helpful to develop relatively simple model systems. One example of this model is going to be presented below. The goal of such models is not necessarily to replicate the usually very complex biological reality, but to create controlled environments that can teach us about the basic principles that may be in common to all nanoscale, thermal machines.

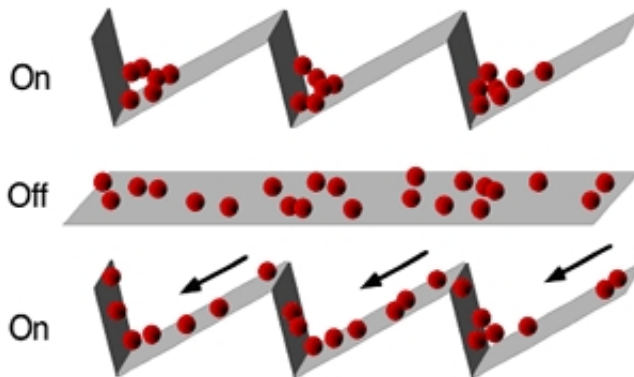


Figure 2: The basic working mechanism of the Brownian motor. Brownian particles are trapped in a periodic, asymmetric potential that can be turned on and off. The random diffusion when the potential is off is converted into net motion to the left when the ratchet is switched on.[15]

## 2.3 Biased Brownian motion

First more general principle that runs Brownian motion should be discussed, before we introduce a model that has been used to study basic principles of Brownian motors. And that principle is biased Brownian motion.

The basic physical idea is simple: a system that is not in thermal equilibrium tends towards equilibrium. If this system lives in an asymmetric world, then moving towards equilibrium will usually also involve a movement in space. To keep the system moving, we need to perpetually keep it away from thermal equilibrium, which costs energy - this is the energy that drives the motion.[7]

We achieve this by fluctuating temperature[8], some chemical reaction[3], periodically turning on and off some asymmetric potential[3] or by periodic forcing a Brownian particle[4]. The latter is going to be discussed in more detail in chapter 3.

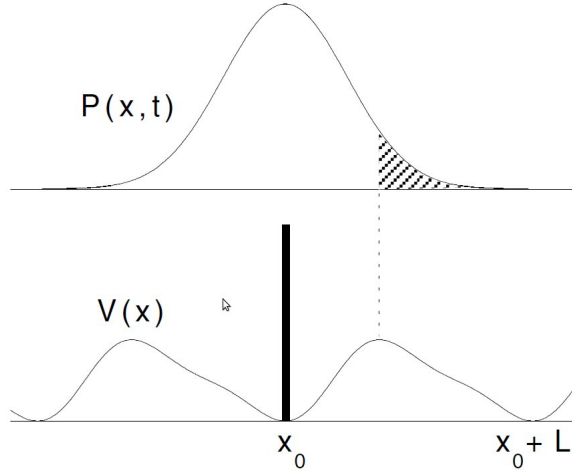


Figure 3: The figure illustrates how Brownian particles, initially concentrated at  $x_0$  (lower panel), spread out when the potential is turned on. When the potential is turned off again, most particles are captured again in the basin of attraction of  $x_0$ , but also substantially in that of  $x_0 + L$  (hatched area). A net current of particles to the right results.[4]

All this processes can be described by inducing some external potential  $U(x)$  in the system. In the case where our periodic potential  $U(x)$  has exactly one minimum and maximum per period  $L$  as in figure (Fig.3), it is quite obvious that if the local minimum is closer to its adjacent maximum to the right (Fig. 3) a positive particle current,  $\dot{x} > 0$ , will arise. Put differently, it is intuitively clear that when the potential is turned off, particles must diffuse a long distance to the left and only a short distance to the right, yielding a net transport against the steep hill towards the right.

So in devices based on biased Brownian motion, net transport occurs by a combination of diffusion and deterministic motion induced by externally applied time dependent electric fields.

It is important to note that particles of different sizes experience different levels of friction and Brownian motion, an appropriately designed external modulation can be exploited to cause particles of slightly different sizes to move in **opposite** directions.[3]

### 3 Periodic forcing of a Brownian particle

As mentioned before we can induce biased Brownian motion by periodic forcing of a Brownian particle. Specifically we are going to look what happens to a Brownian particle (  $2 \mu m$  diameter polystyrene sphere in water) when forced by infra red optical tweezer, that is moving in a circle.

---

<sup>0</sup>Whenever claims in this chapter (Ch. 3) are made but not shown, they should be referenced to[4].



### 3.1 Experimental setup

Suspension of  $2\ \mu\text{m}$  diameter polystyrene spheres are diluted in pure water. They are observed under the microscope, where typically only a few samples of spheres are seen in the field of view ( $50 \times 50\ \mu\text{m}^2$ ).

Image is recorded with CCD camera. Spatial resolution is  $0.1\ \mu\text{m}$ . Pixel intensity on the image is thresholded around the mean value. X and Y coordinates of center of mass are deduced from intensity distribution. Particles never goes out of focus when running the experiment so the Z coordinate is not recorded. Motion of particle is confined to the 2D space.

Laser with wavelength of 1064 nm and transverse Gaussian profile is inserted into the microscope's optical path via the beam splitter. With the help of some optical elements we achieve circular motion of the beam.

### 3.2 Optical trap

The optical trap is based on the transfer of momentum between the beam of radiation and the object that it is passing through. The photons of the beam refract as they pass between the boundary separating object and medium. This refraction results in a force that effectively traps the particle in a 3D environment. However, the outcome of this interplay is dependent on the relationship between the index of refraction ( $n_{obj}$ ) of the object and its relation to the  $n_{env}$  of the environment it is immersed in.[10] In our case the the refractive index of the polystyrene sphere is larger than the water index.[4] Particle is thus attracted to high electric field regions towards the beam axis.

The beam is focused to a sharp focal point inside the sample via microscope lens. The forces are shown in figure (Fig.4). The gradient forces localize the particle to the focal point and the radiation pressure pushes the particle along the beam axis. When the gradient forces overcome the radiation pressure, the beam focal point becomes a trap, an optical tweezer, for the polystyrene sphere. The strength of the trap depends linearly on the output laser power.[4]

### 3.3 Maximum trapping force

Maximum trapping force is measured by moving the sample in a direction transverse to the optical axis. The particle escapes when the sample velocity is such that the Stokes force exceeds the trapping force. This is critical velocity  $V_c$ . We get maximum trapping force from Stokes force ( $F_s = 6\pi\eta aV_c$ ), where  $\eta$  is the room temperature water viscosity and  $a$  the particle radius. The value of the force is of the order of 1 pN for an output laser power of 150 mW. Another measure of the potential and thus force is obtained by observing the fall into the trap (for an output laser power of 150 mW). Potential is plotted on the figure (Fig.5). The depth of the potential is  $250\ k_bT$  for an output laser of 150 mW.

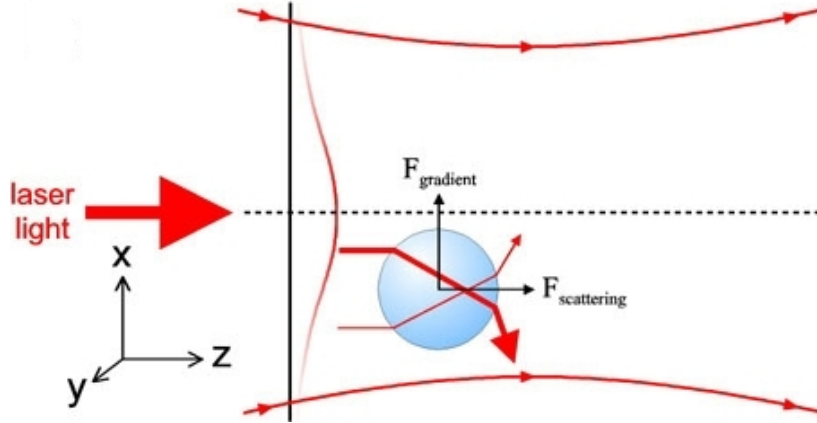


Figure 4: As the beam passes into the bead, it is refracted away from the incident beam axis ( $z$ -axis). This results in a transfer of momentum from the deflected photons to the bead itself. This results a force. The force points in the opposite direction of the change in momentum of the light. It can be broken in two components. The first is parallel to the original direction of the beam. This is the scattering force  $F_s$ , and it can be thought of as the force the particle exerts as it hits the bead. The second component,  $F_{gradient}$  is perpendicular to the scattering force. And when index of refraction of the bead is larger than the water index, then  $F_{gradient}$  localize the particle to the focal point.[16]

### 3.4 Particle dynamics

We mentioned before that our laser tweezer is moving in a circular path.

A typical trajectory recorded in the experiment is shown in figure (Fig.6a). The particle radial excursions are small compared to the circle diameter ( $< 3\%$ ) and to the particle diameter ( $< 20\%$ ). Thus an approximation is made, that particle motion is one dimensional and confined to the circle. We denote the trap rotation frequency by  $\nu_T$ . An average on periods of the order 400 s is done to get well defined mean angular frequency of the particle  $\nu_P$ .

Now we can inspect  $\nu_P$  as a function of  $\nu_T$ . That dependence is plotted in figure (Fig.7) on a logarithmic scale for different output laser powers. Each curve presents three distinct regimes: a phase-locked regime where the particle rotates synchronously with the trap. A phase-slip regime starting first with a very sharp decrease of  $\nu_P$  followed by the power law  $\nu_P \propto \nu_T^{-1}$  and finally a third regime where the particle's motion along the circle is diffusive, the mean angular frequency  $\nu_P$  is zero and not plotted here.

Let us now describe in more detail the curve corresponding to a potential depth of  $1250 k_b T$  (output laser power 700 mW).

#### 3.4.1 Phase-Locked regime

For  $\nu_T$  smaller than 5 Hz (regime I), the particle is trapped and follows the tweezer. The Stokes force is smaller than the maximum trapping force. So the particle stays trapped and

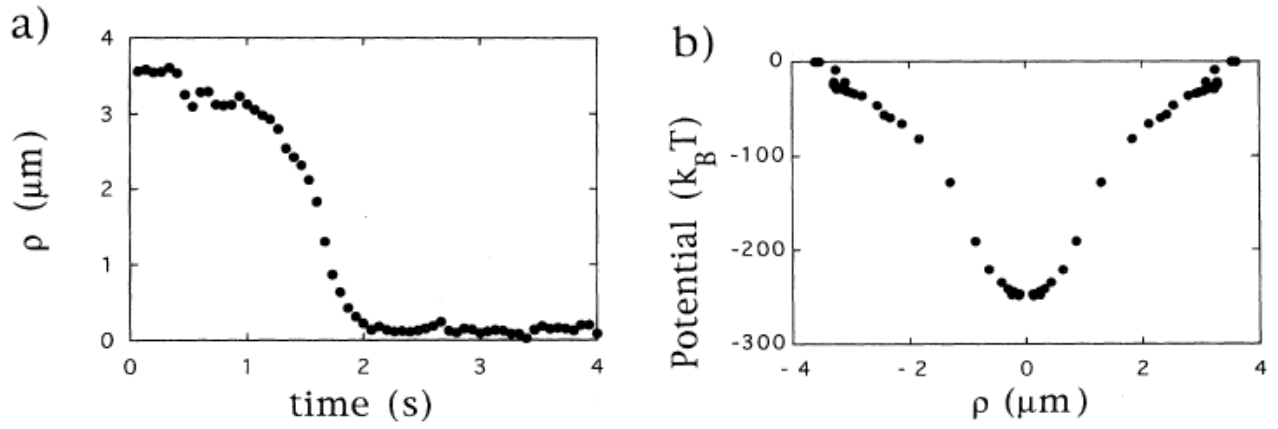


Figure 5: (a) Time series of horizontal displacement of a particle falling into the optical trap. The trap is fixed at the origin. (b) Trapping potential in units of  $k_B T$  for a  $2 \mu\text{m}$  diameter polystyrene sphere. The X axis represents the relative horizontal distance between the particle's center of mass and the beam focal point. Output laser power of 150 mW.[4]

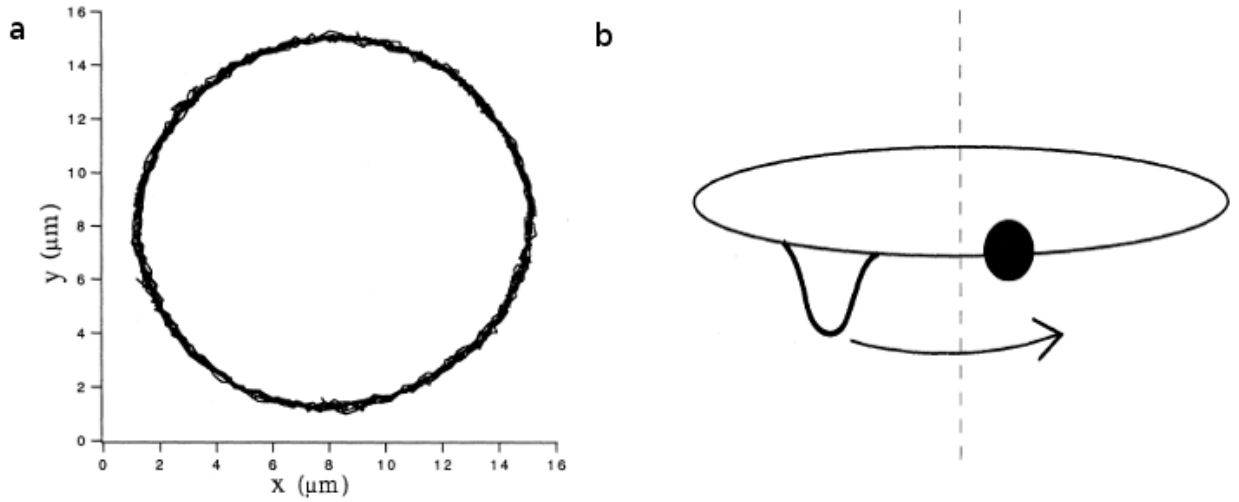


Figure 6: (a) Trajectory of the particle's center of mass. Recording time 60 s. Trap rotating frequency 14 Hz. Output laser power 700 mW. (b) Optical trap is rotating along a circle of a diameter  $12.4 \mu\text{m}$ [4]

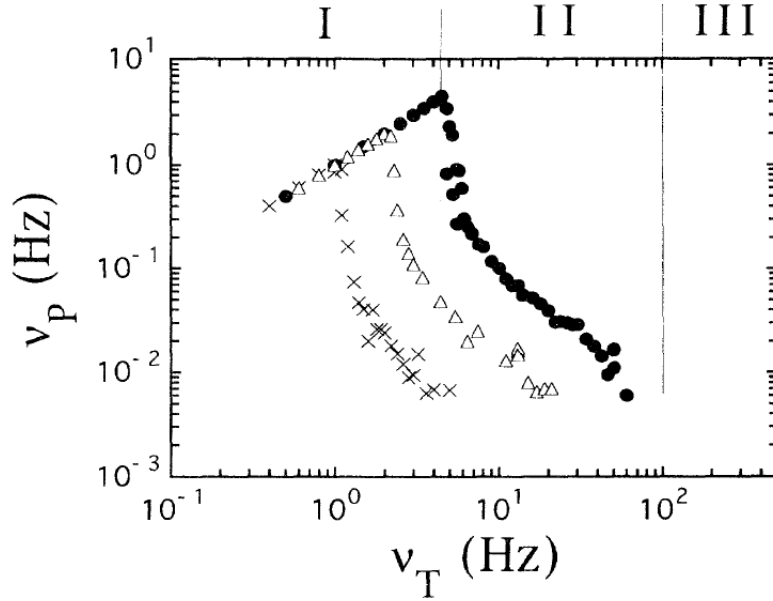


Figure 7: The particle's mean angular frequency  $\nu_P$  as a function of the trap angular frequency  $\nu_T$ . For different output laser power: circles 700 mW, triangles 300 mW and crosses 150 mW.[4]

its angular frequency is  $\nu_T$ . This is indicated by the power law of exponent one in figure (Fig.7).

### 3.4.2 Phase-slip regime

The phase-locked regime disappears when reaching a trap rotation frequency higher than the critical frequency  $\nu_C = 5\text{Hz}$ . The critical particle velocity is then  $V_c = 2 * \pi * R * \nu_C \approx 190\mu\text{m}\cdot\text{s}^{-1}$ . It agrees with the value obtained when we measured maximum trapping force. In this regime the trap is not strong enough to hold the particle, but kicks it regularly at each revolution. Between kicks the particle diffuses, but does not have enough time to diffuse away from circle before the return of the trap. The particle mean angular frequency decreases with the trap frequency. The kicking rotor becomes less and less effective. Just above the critical frequency  $\nu_C$  is a sharp decrease of  $\nu_P$ . In this region,  $\nu_T$  is small enough that one can observe individual trapping and escape events of the particle from the moving trap.

### 3.4.3 Diffusive regime

Since the kick amplitude decreases with  $\nu_T$ , it will eventually become smaller than  $k_bT$  and thermal effects will dominate the particle's motion, at least on small time scale. This happens for frequencies larger than 70 Hz, for an output laser power of 700 mW. What happens in this regime is that particle is still confined in the radial direction because it always experiences the same side of the optical trap when displaced away from the circle, just like in the previous regimes. But in the azimuthal direction it experiences both sides of the trapping potential.

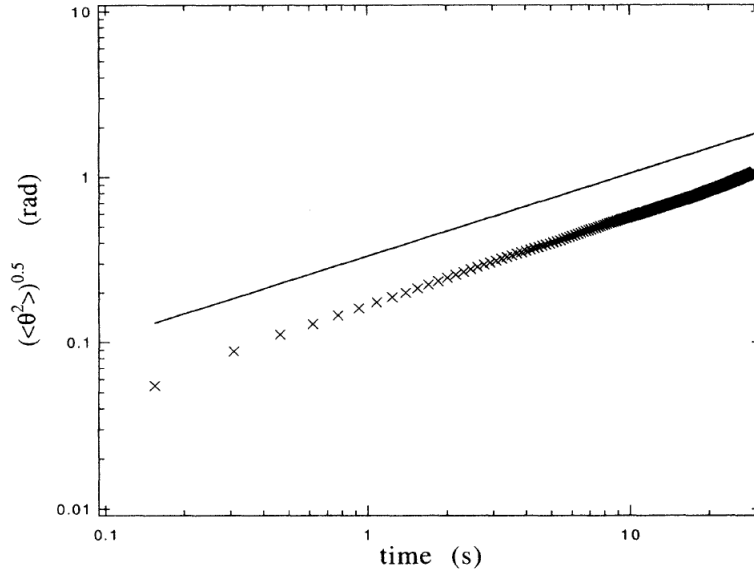


Figure 8: The root mean square value of the particle angular displacement as a function of time, trap rotation frequency 100 Hz, output laser power 700 mW. The straight line indicates a power law with exponent  $\frac{1}{2}$ . [4]

The particle is essentially free to diffuse along the circle. The particle's mean angular velocity is zero.

The figure (Fig.8) shows the root mean square value of the angular displacement as a function of time for  $\nu_T = 100\text{Hz}$ . The straight line is a power law of exponent 1/2, as we know that indicates that the motion is diffusive. Fitting a square root to the experimental points, the angular diffusion constant is  $D_\theta = 0.008\text{rad}^2\text{s}^{-1}$ . The theoretical particle diffusion constant is  $D = \frac{k_B T}{6\pi\eta a} = 0.2\mu\text{m}^2\text{s}^{-1}$ . The trap circular trajectory has a radius R of  $6.2\mu\text{m}$ , thus one estimates  $D_\theta \approx D/R^2 \approx 0.006\text{rad}^2\text{s}^{-1}$ . That is consistent with our previous estimation. Figure (Fig.8) also shows that the particle's motion is diffusive over 30 s only. Long time motions are still sensitive to drifts, however small.

## 4 Langevin equation-Stochastic Differential Equations

A theory has been developed that is consistent with our experimental data. Firstly we will show how Langevin constructed his theory about the motion of a Brownian particle. And then we will associate it with our experimental data.

Langevin began by simply writing down the equation of motion of the Brownian particle according to Newton's laws under the assumption that the Brownian particle experiences two forces[1], namely:

- (i) a fluctuating force that changes direction and magnitude frequently compared to any other time scale of the system and averages to zero over time,
- (ii) a viscous drag force that always slows the motions induced by the fluctuation term.

The advantages of this formulation of the theory are that: In general Langevin's method is far easier to comprehend than the Fokker-Planck equation as it is based directly on the concept of the time evolution of the random variable describing the process rather than on the time evolution of the underlying probability distribution.[1]

Thus, his equation of motion, according to Newton's second law of motion, is [1]

$$m \frac{d^2 x(t)}{dt^2} = -\zeta \frac{dx(t)}{dt} + F(x, t) + f(t)_{stoch} \quad (20)$$

$F(x,t)$  is a term representing some optional external force. The friction term  $-\zeta\dot{x}$  is assumed to be governed by Stoke's law which states that the frictional force decelerating a spherical particle of radius  $a$  is

$$-\zeta\dot{x} = 6\pi\eta a\dot{x} \quad (21)$$

where  $\eta$  is the viscosity of the surrounding fluid. The following assumptions are made about the fluctuating part  $f(t)_{stoch}$ [1]:

- (i)  $f(t)_{stoch}$  is independent of  $x$
- (ii)  $f(t)_{stoch}$  varies extremely rapidly compared to the variation of  $x(t)$
- (iii) The statistical average over an ensemble of particles,  $\overline{f(t)_{stoch}} = 0$ , since  $f(t)_{stoch}$  is so irregular.

In order to describe our experiment we take an arbitrarily shaped potential, moving at a velocity  $V_T$ . The potential and particle motion are one dimensional. The potential has a finite range  $[X_a, X_b]$  and is attractive ( $U < 0$ ), such that  $U(X_a)=U(X_b)$ . In other words, the spatial average of the force is zero. This potential is associated with the force  $F(x,t)$ :

$$F(x, t) = (-\partial/\partial x)U(x, t)$$

**In a deterministic limit** we neglect stochastic forcing  $f(t)_{stoch}$  and we can also show that for physical parameters as in this experiment inertial term is negligible[4]. Then the equation becomes

$$m\zeta\dot{x} = F(x, t) = F(x - V_T t) \quad (22)$$

The potential moving along the  $x$  axis with a velocity  $V_t$  induces a displacement  $\Delta x$  of the particle during a time  $\Delta t$ . Before and after the particle is at rest.

Now we can go to the referential frame, where the potential is fixed. The new position variable is  $y = x - V_T t$ . Equation of motion becomes  $dy = dt\{[F(y)/m\zeta] - V_T\}$ .

It can be shown that  $\Delta x$  is positive in this deterministic limit[4]. This means that the particle is always displaced in the direction of the moving potential, regardless of the potential shape. But we obtain the opposite result in the conservative case.[4]

It can also be shown that asymptotic behaviour is in agreement with our previous statement that  $\nu_P \propto \nu_T^{-1}$  [4]. All this statements have been made for an arbitrary potential.

Now we turn to a specific potential shape. We approximate the bell-shaped potential in figure (Fig.5) by triangular symmetric potential. When we solve equation (Eq.22) for triangular potential we obtain for particle angular frequency: [4]

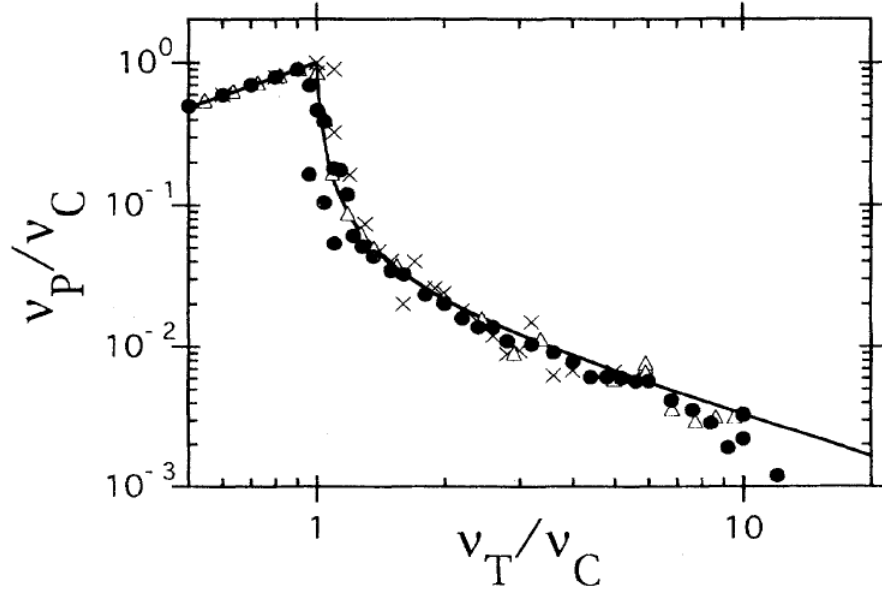


Figure 9: The non dimensional ratio ( $\nu_P/\nu_C$ ) as a function of ( $\nu_T/\nu_C$ ). The output laser is 700 mW (circles), 300 mW (triangles) and 150 mW (crosses). The solid line is computed from equation (Eq.23),  $X_0 = 0.6\mu m r$

$$\frac{\nu_P}{\nu_C} = \left[ \frac{X_0}{\pi R} \right] \left[ \frac{(\nu_T/\nu_C)}{(\nu_T/\nu_C)^2 - 1} \right] \left[ 1 + \frac{(X_0/\pi R)}{(\nu_T/\nu_C)^2 - 1} \right]^{-1} \quad (23)$$

The solid line in figure (Fig.9) represents the computed values from equation (Eq.23). We can see a very good agreement between experiment and the theory we developed above. We can also justify neglected thermal noise term. That is quite surprising given the stochastic character of the actual trajectories.

But it is not surprising since the potential depth is larger than  $250 k_b T$  for an output laser power of 150 mW. However under this condition the first moment of a trajectory even stochastic is still deterministic.

## 5 Fokker-Planck equation

The Fokker-Planck equation is just an equation of motion for the distribution function of fluctuating macroscopic variables[11].The diffusion equation (Eq.7) for the distribution function of an assembly of free Brownian particles is a simple example of such a equation.[11]

The main use of the Fokker-Planck equation is as an approximate description for any Markov process in which the individual jumps are small[9]. For derivation of Fokker-Planck equation (Eq.24) look at [1].

$$\frac{\partial \rho(y, t|x)}{\partial t} = -\frac{\partial}{\partial y} [D_1 \rho(y, t|x)] + \frac{\partial^2}{\partial y^2} [D_2 \rho(y, |x)] \quad (24)$$

$D_1$  is called drift coefficient and  $D_2$  is called diffusion coefficient.

The FokkerPlanck equation describes the time evolution of the probability density function of the position of a particle, and can be generalized to other observables as well.[1] With the help of this equation we can study the effect of temperature.[11]

We get the value of drift coefficient  $D_1 = F(y) - m\gamma V_T$  out of Langevin equation.[1] And Einstein told us what diffusion coefficient is  $D_2 = k_B T/m\gamma$ .

Here we introduce the probability current  $j(y,t)$  (Eq.25) so we can write the Fokker Planck equation in simpler form (Eq.26).

$$j(y, t) = \frac{\rho(y, t)}{m\gamma} [F(y) - m\gamma V_T] - \frac{k_B T}{m\gamma} \frac{\partial}{\partial y} \rho(y, t) \quad (25)$$

$$\frac{\partial}{\partial t} \rho(y, t) = -\frac{\partial}{\partial y} j(y, t) \quad (26)$$

where  $\rho$  is the probability density of the particle and  $j(y,t)$  is the probability current.

We are interested in stationary solutions for  $\rho(y, t)$  so we set to zero the left hand side of equation (Eq.26). The current  $j(y,t)$  is then constant in time. The steady state solution is then also a general solution of equation (Eq.25).

$$\rho(y) = \left[ C - \frac{j m \gamma}{k_B T} \int_0^y dy' \exp \left( \frac{U(y') + m \gamma V_T y'}{k_B T} \right) \right] * \exp \left( -\frac{U(y) + m \gamma V_T y'}{k_B T} \right) \quad (27)$$

Because the trap motion occurs on a circle of radius  $R$ , we set the stationary probability density  $\rho(y)$  to be periodic of period  $L = 2\pi R$ . This implies a relation between the particle current  $j$  and the constant  $C$ . When we insert this relation back into expression of  $\rho(y)$  we get

$$\rho(y) = \frac{j m \gamma}{k_B T} \left( 1 - \exp \left[ \frac{m \gamma V_T L}{k_B T} \right] \right)^{-1} * \int_0^L dy' \exp \left[ \frac{U(y + y') - U(y) + m \gamma V_T y'}{k_B T} \right]. \quad (28)$$

Now we demand that probability density  $\rho(y)$  is normalized to 1. That yields

$$\frac{k_B T}{j m \gamma} \left( 1 - \exp \left[ \frac{m \gamma V_T L}{k_B T} \right] \right) = \int_0^L dy \int_0^L dy' \exp \left[ \frac{U(y + y) - U(y) + m \gamma V_T y'}{k_B T} \right]. \quad (29)$$



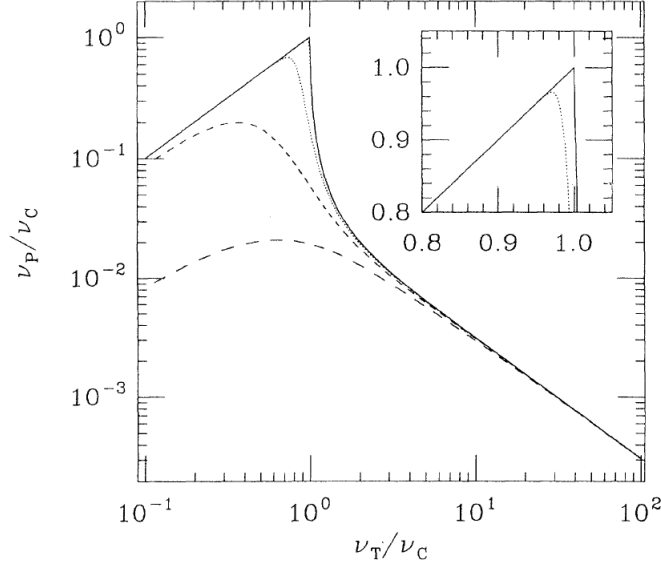


Figure 10: The ratio  $(\nu_P/\nu_C)$  as a function of  $(\nu_T/\nu_C)$ , for different temperatures. The solid line (T=0 K) is from equation (Eq.23). The dashed are computed from equation (Eq.29) for T=300 K,3000 K,10000 K and 30000 K.

The above equation (Eq.29) relates the particle current  $j$  to the physical parameters of our system. The potential  $U(y)$ , the trap velocity  $V_t$ , and the temperature  $T$ .

The mean value of the particle velocity in the referential frame, where the potential is fixed is simply  $V_P = jL$ . In the absence of potential, this mean velocity would be  $V_P = -V_T$ . The presence of force delays the motion of the particle and induces a positive drift  $\Delta V = V_P + V_T$  whatever the referential frame. The mean angular frequency of the particle is then given by  $\nu_P = \frac{\Delta V_P}{2\pi R}$ .

Now we take the trapping potential to be triangular as before. For such a potential, one can solve equation (Eq.29) analytically for the probability current  $j$  and the particle rotation frequency  $\nu_P$ .

The solution for  $\frac{\nu_P}{\nu_C}$  is shown in figure (Fig.10) for different temperatures. The curve for T=0 K (solid line) is computed from deterministic model. The room temperature T=300 K is almost indistinguishable from the deterministic one. The almost complete agreement between the two curves explains why the deterministic model is so powerful in describing the experimental behaviours. The potential depth is so large compared to the noise, that the temperature can be set to zero when computing the particle's rotation frequency.

The end result for  $\nu_P$  depends only on  $m\gamma V_T/k_B T$  and  $m\gamma V_C/k_B T$ . Thus reducing the potential depth (and therefore  $V_C$ ) is equivalent to increasing the temperature. Curves at higher temperatures (T= 3000, 10000 and 30000 K) are also plotted in figure (Fig.10) to illustrate the effect of thermal noise on  $\nu_P$ .

$\nu_P$  always decreases when T increases. The kicking rotor becomes less efficient when more noisy[4]. Also, as  $\nu_T$  goes to infinity, all curves collapse on the asymptotic scaling discussed before.

## 6 Conclusion

We described motion of a single Brownian particle and we discovered that there are three regimes of motion that are characteristic for a noisy asynchronous rotor. The experiment typically involves only one particle, so the motion is not hard to understand and it is relatively easy to describe it with mathematical formula. The usefulness and *beauty* of this experiment is that we can generalize its discoveries to other more complicated systems.

The use of noise in technological applications is still in its infancy, and it is far from clear what the future holds. Nevertheless, there is already much active research in the area of noise enhanced magnetic sensing [12] and electromagnetic communication [13]. The recent work on fluctuation driven transport leads to optimism that similar principles can be used to design microscopic pumps and motors, machines that have typically relied on deterministic mechanisms involving springs, cogs, and levers. Such devices would be consistent with the behaviour of molecules, including enzymes, and could pave the way to construction of true molecular motors and pumps.[3]

## 7 References

- [1] W.T. Coffey, Yu. P. Kalmykov, J. T. Waldron, The Langevin equation (World Scientific, Singapore, 1998)
- [2] M. D. Haw: Einstein's random walk, Physics World, January 2005
- [3] R. D. Astumian: Thermodynamics and kinetics of a Brownian motor, Science 276, p. 917-922 (1997)
- [4] L. P. Faucheux and A. J. Libchaber, Periodic forcing of a Brownian particle, Phys. Rev. E 49, 5158 (1994)
- [5] [http://en.wikipedia.org/wiki/Brownian\\_motor](http://en.wikipedia.org/wiki/Brownian_motor) (4.1.2010)
- [6] P. Reimann, P. Hänggi, Introduction to the physics of Brownian motors, Appl. Phys. A 75 (2002) 169
- [7] [http://www.uoregon.edu/linke/res\\_ratchet.html](http://www.uoregon.edu/linke/res_ratchet.html) (1.4.2010)
- [8] Li Yu-xiao, Biased Brownian Motion Driven by Fluctuating Temperature, Chinese Phys. Lett. 14 332-335 (1997)
- [9] [http://en.wikipedia.org/wiki/FokkerPlanck\\_equation](http://en.wikipedia.org/wiki/FokkerPlanck_equation) (4.1.2010)
- [10] Optical trap guide, [http://physics.ucsd.edu/neurophysics/courses/physics\\_173\\_273/optical\\_trap\\_guide.pdf](http://physics.ucsd.edu/neurophysics/courses/physics_173_273/optical_trap_guide.pdf) (2010)
- [11] H. Risken, The Fokker-Planck equation (Springer-Verlag, Berlin, 1996)
- [12] A. Hibbs et al., J. Appl. Phys. 77, 2582 (1995); R. Rouse, S. Han, J. Luckens, Appl. Phys. Lett. 66, 108 (1995)
- [13] V. S. Anishchenko, M. A. Safanova, L. O. Chua, Int. J. Bifurcation Chaos 4, 441 (1994)
- [14] [http://www.scienceisart.com/A\\_Diffus/DiffusMain\\_1.html](http://www.scienceisart.com/A_Diffus/DiffusMain_1.html) (4.1.2010)
- [15] [http://www.uoregon.edu/linke/images/research\\_flashingratchet.gif](http://www.uoregon.edu/linke/images/research_flashingratchet.gif) (4.1.2010)
- [16] <http://www.stanford.edu/group/blocklab/OpticalTweezersIntroduction.htm> (4.1.2010)